Laboratory of Nuclear Studies, Cornell University

August, 2001 CBN 01-15

Modification of TEAPOT to Handle Acceleration/Deceleration in the ERL

Richard Talman

ABSTRACT

To analyse the energy recovery linac (ERL) it is essential to develop codes that combine linac and storage ring formalisms. This is a first draft of documention describing a linac capability for TEAPOT, which has previously been used only for circular rings that are static, or at most have slow energy ramping. Standing wave, π-mode, linac operation is assumed.

For the time being the report includes considerable argumentative material concerning the Rosenzweig and Serafini "ponderomotive" formalism. Comparing their formulas with the result of numerical integration of the equation of transverse motion, I find their ponderomotive correction to be completely wrong except when it is negligible (which it is in all but the early sections of the ERL linac.) This material will be excised, or at least greatly abbreviated, once there is an agreed-upon understanding of the issues.

To illustrate code capability, optics are exhibited for a complete acceleration/recirculation/deceleration cycle in the Cornell ERL. (Except in the first RF cavity) there is satisfactory agreement with the results of Bazarov, though an exact comparison has not yet been possible.

Technical details concerning the TEAPOT implementation and its relation to PARMELA are appended.

1. Introduction

The following two figures show optics as calculated, for similar, but not identical ERL configurations, by Ivan Bazarov's[1] program above, and by TEAPOT[2] below.

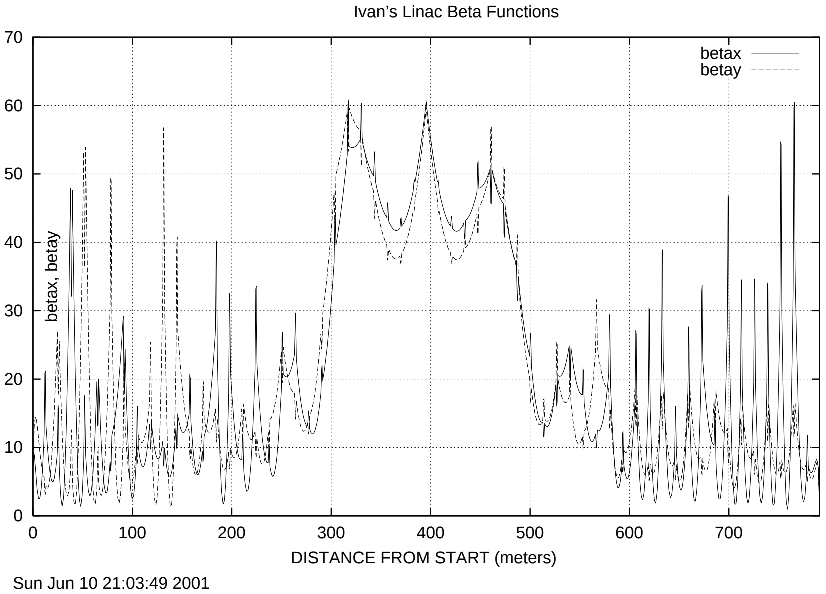

Figure 1.1: Bazarov's beta functions for acceleration and deceleration through the ERL linac. Initial Twiss parameters fit empirically; $\beta_x = 7.32\,\mathrm{m}$, $\alpha_x = -3.36$, $\beta_y = 7.50\,\mathrm{m}$, $\alpha_y = -5.08$.

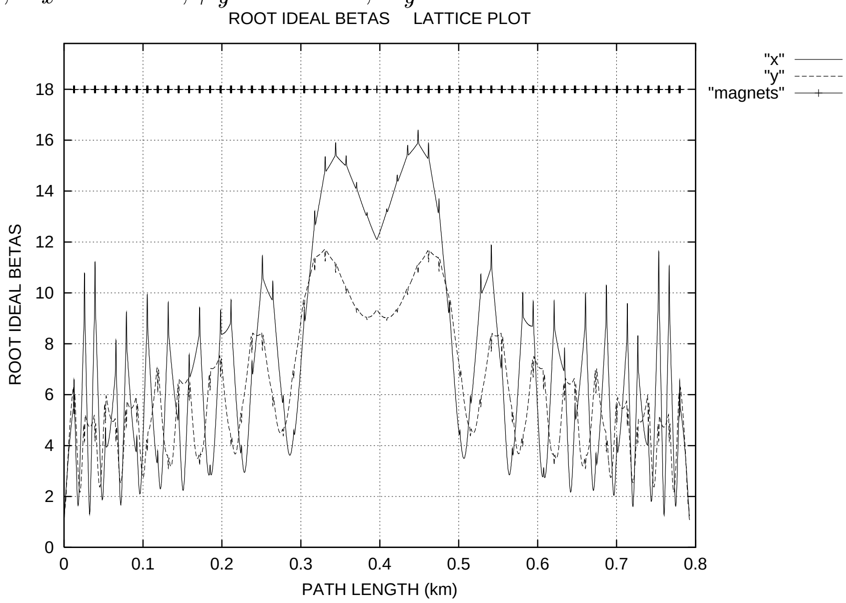

Figure 1.2: TEAPOT beta functions for acceleration and deceleration through the ERL linac. Initial Twiss parameters fit by periodic match; $\beta_x = 1.15\,\mathrm{m}$, $\alpha_x = -0.096$, $\beta_y = 1.53\,\mathrm{m}$, $\alpha_y = -0.051$.

The following introductory comments/rationalizations can be made:

- The general trends are consistent.
- The maximum TEAPOT beta functions are as much as 4 times greater. (Note the different vertical scales.) Even if this remains true (reasons are given why it won't) the ERL emittances may be small enough to tolerate the TEAPOT values. The worst disagreement is in the region where the (absolute) emittances are minimum.
- The initial Twiss values (see figure captions) disagree, but are at least in the same ball park. There is no reason why they should agree exactly anyway, as they are determined differently. Since the injection energy is 10 MeV the more difficult task of discussing the non-relativistic gun section is not even begun. It remains to be seen whether either set of injection Twiss values is achievable with practical gun design.
- Ivan's triplet strengths were chosen to minimize the maximum betas; mine were just chosen to fall monotonically along the linac. This could plausibly account for a factor of two of the discrepancy.
- In this particular lattice figure Ivan has not bothered to match from acceleration output to deceleration input. In his 17 March 2001 note "First-Order Turnaround Optics in 5 GeV ERL", Ivan exhibits matching optics in which the peak horizontal beta function has a maximum of 90 m. This accounts for another factor of 1.5 of the discrepancy.
- It is very likely that the only important beta function discrepancy is launched at the low energy end and propagates to the high energy end. The fact that the Cornell ERL will have two orders of magnitude greater output/input energy ratio than, say, the Jefferson lab FEL, greatly magnifies effects that might not have been noticeable at J-lab.

The remaining sections discuss details of these trajectory calculations.

2. Logarithmic Trajectory Formalism

For a fully relativistic electron traveling in synchronism with the field in a linac, the forces acting on the electron can be expressed as pure functions of the electron's longitudinal position z. This makes it possible, in principle, to treat the electron trajectory using the standard Courant-Snyder, time-independent formalism. The longitudinal field in a standing wave linac, with first cavity center at $z = 0$ and peak longitudinal field $\hat{E}_z$, is given by

$$E_z\,(t, z) = \hat{E}_z\,\cos\omega_{\mathrm{RF}}t\,\cos k_{\mathrm{RF}}z\ , \tag{2.1}$$

Consider an electron for which

$$z = ct + z_\phi, \quad \text{or} \quad \omega_{\mathrm{RF}}t = k_{\mathrm{RF}}z + \phi, \quad \text{where} \quad \phi = -k_{\mathrm{RF}}z_\phi \tag{2.2}$$

Expressed in terms of the electron's location z the longitudinal field is

$$E_z\,(z) = \hat{E}_z\,\cos\left(k_{\mathrm{RF}}z + \phi\right)\,\cos k_{\mathrm{RF}}z = \hat{E}_z\,\cos\phi\,\cos^2 k_{\mathrm{RF}}z - \hat{E}_z\,\sin\phi\,\cos k_{\mathrm{RF}}z\,\sin k_{\mathrm{RF}}z\ . \tag{2.3}$$

Since the final term integrates to zero across each cavity, it gives no net contribution to the particle acceleration. Hence, for energy gain we can use

$$E_z\,(z) = \hat{E}_{z,\phi}\,\cos^2 k_{\mathrm{RF}}z, \quad \text{where} \quad \hat{E}_{z,\phi} = \hat{E}_z\,\cos\phi\ . \tag{2.4}$$

In practice the different cavities of a linac need not be exactly in phase, in which case ϕ depends on z. Even though it is straightforward in principle to account for this dependence, it is tedious in practice. So let us assume that ϕ is constant for the present discussion.

We will concentrate on propagation from one node to the next, a length equal to $\lambda/2 \equiv \pi/k_{\mathrm{RF}}$, that will also be known as "the cavity". (Usually there will be multiple cavities, with the end of one coincident with the start of the next one.) To enable conventional lattice calculations it will be convenient to approximate the sinuisoidally varying field by a field that is uniform and time-independent, with value $E_{z,\mathrm{unif.},\phi}$, over a shorter length $\Delta z = z_1 - z_0$ (which will be approximately $\lambda/4$).† Equating energy gains, since the average value of $\cos^2$ is $1/2$, we obtain‡

$$E_{z,\mathrm{unif.},\phi}\Delta z = \frac{\hat{E}_{z,\phi}}{2}\,\frac{\lambda}{2} = \frac{\langle \mathcal{E}'_\phi \rangle}{-e}\,\frac{\lambda}{2}\ , \tag{2.5}$$

† Because the longitudinal field profile resembles architectural "dentils", that is what it will be called.

‡ All formulas are applicable to either electrons or positrons, but for simplicity electrons will always be assumed, so the charge is -e.

where $\langle \mathcal{E}'_\phi \rangle$ is the average energy gain per unit length while in the standing wave. Taking $z = 0$ at the cavity center, the points $z_{0,1}$ will locate the "effective" entry and exit planes. These dimensions are shown in Fig. 2.1. While in this "effective cavity" the energy is assumed to vary from $\mathcal{E}_0$, its value on entry, according to

$$\mathcal{E}_\phi\,(z) = \mathcal{E}_0 + \langle \mathcal{E}'_\phi \rangle \,\frac{\lambda/2}{\Delta z}\,(z - z_0) \tag{2.6}$$

The notation here is intentionally unsymmetric; $\mathcal{E}_0$ has no ϕ subscript while $\mathcal{E}_\phi(z)$ does. When the electron arrives at a cavity entrance its energy depends on its phase as it passed through earlier cavities, but this dependence is now suppressed. On the other hand the energy evolution in the present cavity depends on ϕ and this dependence is emphasized explicitly by the notation. This notation may be somewhat helpful in generalizing the formulas when ϕ, in fact, varies from cavity to cavity.

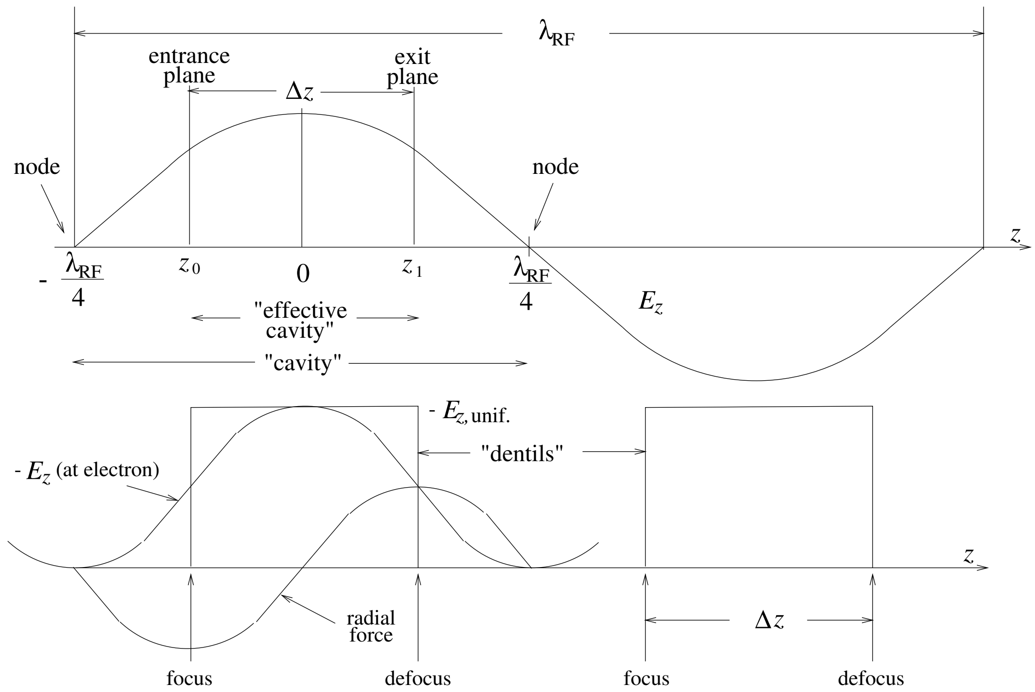

Figure 2.1: Terminology relating cavity structure to longitudinal standing wave for *on-crest* operation. The lower figure shows fields at the electron's instantaneous position and and replacement of accelerating field by a train of uniform field "dentils" or "teeth" of thickness $\Delta z \approx \lambda/4$. The radial force is replaced by delta functions at every entrance and exit. This is the model implemented in TEAPOT.

Everywhere in the structure the transverse momentum, say the x-component, is conserved;

$$\frac{dp_x}{dt} = 0. \tag{2.7}$$

Using $dz = c\,dt$ this can be written in terms of total energy $\mathcal{E}_\phi$,

$$\frac{d}{dz}\left(\mathcal{E}_\phi\,(z)\,\frac{dx}{dz}\right) = 0, \tag{2.8}$$

which integrates to

$$dx = \text{const}\,\frac{dz}{\mathcal{E}_\phi\,(z)} = x_0'\,\frac{dz}{1 + \frac{\langle\mathcal{E}_\phi'\rangle}{\mathcal{E}_0}\,\frac{\lambda/2}{\Delta z}\,(z - z_0)} \tag{2.9}$$

where x_0' is the slope of a particle at $z = z_0$. Integrating this equation yields

$$x = x_0 + x_0'\frac{\mathcal{E}_0}{\langle\mathcal{E}_\phi'\rangle}\,\frac{\Delta z}{\lambda/2}\,\ln\left|1 + \frac{\langle\mathcal{E}_\phi'\rangle\frac{\lambda/2}{\Delta z}}{\mathcal{E}_0}\,(z - z_0)\right|\,. \tag{2.10}$$

While the electron is within the effective cavity this trajectory can be fit artificially by a straight line trajectory with slope adjusted to give the correct output position;

$$x_1 = x_0 + x_0'\,\frac{\mathcal{E}_0}{\mathcal{E}_{1,\phi} - \mathcal{E}_0}\,\ln\frac{\mathcal{E}_{1,\phi}}{\mathcal{E}_0}\,\Delta z = x_0 + x_0'\,L_{\text{eff.}} \tag{2.11}$$

The effective cavity therefore appears to have an effective length given by†

$$L_{\text{eff.}} = \frac{\mathcal{E}_0}{\mathcal{E}_{1,\phi} - \mathcal{E}_0}\,\ln\frac{\mathcal{E}_{1,\phi}}{\mathcal{E}_0}\,\Delta z \quad \left(\approx \frac{\mathcal{E}_0}{\mathcal{E}_{1,\phi} - \mathcal{E}_0}\,\ln\frac{\mathcal{E}_{1,\phi}}{\mathcal{E}_0}\,\frac{\lambda}{4}\right), \tag{2.12}$$

where the result in parenthesis comes from setting $\Delta z \approx \lambda/4$. The actual exit slope is

$$x_1' = x_0'\frac{\mathcal{E}_0}{\mathcal{E}_{1,\phi}}\,, \tag{2.13}$$

as can be seen from the first of Eqs. (2.9) The value of the Jacobean is

$$J\left(\frac{x_1, x_1'}{x_0, x_0'}\right) = \frac{\mathcal{E}_0}{\mathcal{E}_{1,\phi}}\,. \tag{2.14}$$

† Eqs. (2.12) and (2.13) contain the lion's share of the physics of the so-called "RF focusing". They are what causes the "adiabatic damping" exhibited by Eq. (2.14). But the edge focusing, especially at the first few edges, is important because the particles are least stiff there, and the tuning of all subsequent optics is affected.

3. Aside Concerning Cell-By-Cell Treatment of Linac Sections

Though Eq. (2.12) is here being applied to a single cell, it is often applied to an entire linac for which $\mathcal{E}_{1,\phi}$ is large compared to $\mathcal{E}_0$, in which case $L_{\mathrm{eff.}}$ can be much less than Δz.

When Eq. (2.12) is applied at the low energy end of a linac the result can be internally inconsistent. Consider, for example, the first, nine-cell section of the Cornell ERL, which has total length 1.04 m and increases the electron energy from 10.0 MeV to 30.8 MeV in the nine equal steps exhibited in Table 3.1. The "effective length" of the 1.04 m section as given by Eq. (2.12) is 0.625 m if the section is treated as a single lumped energy increase and as 0.977 m if it is (more correctly) treated as nine increases. Since the beta function evolves according to $\beta(\Delta s) = \beta(0) - 2\alpha(0)\Delta s + \Delta s^2(1+\alpha^2(0))/\beta(0)$, ambiguity in element length is immediately reflected in ambiguity in beta function evolution. Since the beta function values are only a few meters in this region this discrepancy is not at all negligible.

Table 3.1: Energy steps in first section of Cornell ERL.

E_0	MeV	10.01	12.31	14.62	16.93	19.24	21.56	23.87	26.18	28.49	total	10.01
E_1	MeV	12.31	14.62	16.93	19.24	21.56	23.87	26.18	28.49	30.80		30.80
$L_{\mathrm{eff.}}$	m	0.1040	0.1059	0.1073	0.1083	0.1091	0.1098	0.1103	0.1107	0.1111	0.9765	0.6253

More serious than this effective length effect is ambiguity in the treatment of entrance and exit focusing. If the section is treated as nine cavities there are nine focusing lenses with nine defocusing lenses interleaved. Since the "lens powers" depend inversely on energy, adjacent lenses have roughly equal but opposite strengths and their effects tend to cancel. Treating an entire nine-cell section as a single accelerating section greatly exaggerates the focusing effect of the entrance lens. Even in later sections, where the fractional energy increase is much less, because the entrance and exit lenses effectively form a doublet, their effect is artificially enhanced because the strength of a doublet is proportional to the lens separation.

For these reasons TEAPOT will apply Eq. (2.12) only to single cavities in which the fractional energy gain is not great, in which case

$$L_{\mathrm{eff.}} = \Delta z \, \frac{\mathcal{E}_0}{\Delta\mathcal{E}} \ln\left(1 + \frac{\Delta\mathcal{E}}{\mathcal{E}_0}\right) \approx \Delta z \left(1 - \frac{1}{2}\frac{\Delta\mathcal{E}}{\mathcal{E}_0} + \dots\right) \tag{3.1}$$

is only slightly shorter than Δz.

4. Ponderomotive Focusing

So far any slope changes have been due to longitudinal acceleration. But there are *actual* transverse forces on a particle in a z-dependent longitudinal RF field. They modify the transverse evolution analysed in the previous sections. Calculations of their effect have been described by Hartman, Rosenzweig, Serafini, and Stevens, in various combinations. [3–5]

Consider transverse force F_x, which is assumed to be proportional to x. It causes the slope x' to vary with position z;

$$\begin{aligned} \gamma\beta mc\, dx' &= dp_x = F_x\, dt = \frac{dF_x}{dx}\, x\, \frac{dz}{\beta\gamma} \\ \frac{dx'}{dz} &= \frac{F_x}{x\gamma\beta^2 mc^2}\, x \equiv K_x\, x \end{aligned} \tag{4.1}$$

The papers mentioned above consider a longitudinal rf field $E_{\rm rf}$ that causes the particle energy $\mathcal{E}$ to vary as

$$\frac{d\mathcal{E}}{dz} = -e\frac{dV}{dz} = eE_{\rm rf}. \tag{4.2}$$

In a cavity of length L in which the energy increase is $\Delta\mathcal{E}$ one has

$$\Delta\mathcal{E} = e\overline{E_{\rm rf}}\, L \tag{4.3}$$

and they derive a radial (i.e. the same for x and y) focusing force with strength (i.e. $K = F_r/r$) given by

$$K = \frac{1}{2}\left(\frac{e\overline{E_{\rm rf}}}{\gamma mc^2}\right)^2 = \frac{1}{2}\left(\frac{\Delta\mathcal{E}/L}{\mathcal{E}}\right)^2 \tag{4.4}$$

where $\beta \approx 1$ has been assumed. Should one wish to represent the focusing by a thin lens of strength (i.e. inverse focal length) $q = KL$ then

$$q = \frac{L}{2}\left(\frac{\Delta\mathcal{E}/L}{\mathcal{E}}\right)^2 \quad \left(\overset{\text{e.g.}}{=} \frac{1\,\text{m}}{2}\left(\frac{20\,\text{MeV/m}}{10\,\text{MeV}}\right)^2 = 2\,\text{m}^{-1}\right) \tag{4.5}$$

This gives a very strong focusing in the first cell of the linac but rapidly becomes negligible as $\mathcal{E}$ increases.

This "ponderomotive focusing" is said to result because, during the RF-induced oscillation about the orbit the particle would otherwise follow, there is, on average, a force directed toward the cavity centerline. The net focusing force is obtained by averaging over betatron phases. It seems to me that this ponderomotive treatment is made invalid because of illegitimate averaging over RF phases (when the electron, in fact, "rides the crest" of the RF wave) and (even more so) by the large fractional energy change per betatron period in those very few RF sections (at the front end) where the focusing is actually not negligible. In particular this invalidates the L-dependence of Eq. (4.5).

My reading of Hartman and Rosenzweig[4] seems to confirm this when they state, on the second page of their paper, that their calculated force is proportional to "reference position" x_0. In traditional betatron formalism the reference position is $x_0 = 0$ so even their averaged force would vanish for a traditionally-defined, isotropically-populated phase space. H and R seem to further corroborate this when they say "The ponderomotive force is focusing ... because the particle, while oscillating, experiences a slightly larger inward force during the half-cycle it is farther than x_0 from the azis, and a slightly smaller inward force during the opposite half-cycle." Again, since $x_0 = 0$ in traditional betatron formalism, their so-called "ponderomotive" focusing cannot be substituted directly into the Courant-Snyder formalism.

So, in the following sections, for implementation in TEAPOT, I take a different approach that accounts for a focusing effect and a defocusing effect within each "cavity" (i.e. between adjacent nodes of an RF standing wave.) Because of the usual AGS principle these will yield a net focusing effect, which seems to be deserving of the title "ponderomotive focusing". In this way, by proceeding more numerically and refraining from extrapolating over large (relative) energy gains, the problem of ponderomotive focusing can be "finessed".[†]

[†] Rosenzweig and Serafini themselves state (page 1602) that "the averaging technique for the second-order focusing, as well as the derivation of the kick matrices at the ends of the cavities, required that the relative change in the energy over a cell be small."

5. Transverse RF Force

Following Kim[6] and Helm and Miller[7]

the dominant RF field component is $E_z(z,t)$. For small r the azimuthal magnetic field can be approximated by $B_\phi \approx B'_\phi r$, which can be obtained from E_z using

$$\frac{\partial E_z}{\partial\,(ct)} \approx \frac{1}{r}\,\frac{\partial}{\partial r}\,\left(r^2 c B'_\phi\right) = \frac{2}{r}\,cB_\phi\ . \tag{5.1}$$

(The source of this azimuthal field is longitudinal displacement current which induces magnetic circulation satisfying Ampère's law.) Similarly the radial electric field can be approximated by $E_r \approx E'_r r$ which, using the divergence equation, is derived from E_z by

$$\frac{\partial E_z}{\partial z} \approx -\frac{1}{r}\,\frac{\partial}{\partial r}\,\left(r^2 E'_r\right) = -\frac{2}{r}\,E_r\ . \tag{5.2}$$

With electric field given by Eq. (2.1),

$$\begin{aligned}
\frac{\partial E_z}{\partial z} &= -\,k_{\mathrm{RF}}\,\hat{E}_z\,\cos\left(k_{\mathrm{RF}}z+\phi\right)\,\sin k_{\mathrm{RF}}z \\
&= -\,\frac{k_{\mathrm{RF}}}{2}\,\hat{E}_{z,\phi}\,\sin 2k_{\mathrm{RF}}z + k_{\mathrm{RF}}\,\hat{E}_{z,\phi}\,\tan\phi\,\sin^2 k_{\mathrm{RF}}z\ , \\
\frac{\partial E_z}{\partial\,(ct)} &= -\,k_{\mathrm{RF}}\,\hat{E}_z\,\sin\left(k_{\mathrm{RF}}z+\phi\right)\,\cos k_{\mathrm{RF}}z \\
&= -\,\frac{k_{\mathrm{RF}}}{2}\,\hat{E}_{z,\phi}\,\sin 2k_{\mathrm{RF}}z - k_{\mathrm{RF}}\,\hat{E}_{z,\phi}\,\tan\phi\,\cos^2 k_{\mathrm{RF}}z\ .
\end{aligned} \tag{5.3}$$

The radial force on an electron (charge -e) passing through the cavity parallel to the axis with velocity $v \approx c$ is[†]

$$\begin{aligned}
F_r &= -\,e\left(E_r - vB_\phi\right) \\
&= -\,\frac{e\,r\,k_{\mathrm{RF}}}{2}\,\hat{E}_{z,\phi}\,\sin 2k_{\mathrm{RF}}z - \frac{e\,r\,k_{\mathrm{RF}}}{2}\,\hat{E}_{z,\phi}\,\tan\phi\,\cos 2k_{\mathrm{RF}}z\ .
\end{aligned} \tag{5.4}$$

The second term is reduced by the factor $\tan\phi$ which is small for on-crest operation. For the time being, since one cannot really afford to run much off-crest, I will set $\tan\phi = 0$. Then, during acceleration of, say, electrons, since $E_z < 0$, this force is *focusing* on entry, where $z < 0$, and *defocusing* on exit. Apart from the usual "alternating gradient" net focusing of such a pair of lenses, we expect a much stronger net focusing because $\mathcal{E}_{1,\phi} > \mathcal{E}_0$

[†] In Eq. (5.4) one can replace r by, say, x and at the same time F_r by F_x, even though x and r behave differently near the origin; it is valid because F_x and F_r have matching dependencies that validate the replacements. The equation can be applied similarly to y.

which makes the exit focusing relatively weaker. During deceleration, still of electrons, the force is defocusing on input, but this is now the weaker of the forces so the net effect is probably still focusing. (The comments in this paragraph would apply equally to positrons since both the charge and E_z change sign.)

6. The Orbit Differential Equation

With E_z given by Eq. (2.4) the (essentially exact, and certainly more accurate than Eq. (2.6)) z-dependence of particle energy is obtained by adjusting $\hat{E}_z$ to produce the given energy gain $\Delta\mathcal{E}$;

$$-e\hat{E}_z = \frac{4\Delta\mathcal{E}}{\lambda} \tag{6.1}$$

and integating

$$\frac{d\mathcal{E}}{dz} = \frac{4\Delta\mathcal{E}}{\lambda}\cos^2\frac{2\pi\, z}{\lambda} \tag{6.2}$$

to obtain

$$\mathcal{E} = \mathcal{E}_0 + \Delta\mathcal{E}\left(\frac{2}{\lambda}\left(z+\frac{\lambda}{4}\right) + \frac{1}{2\pi}\sin\frac{4\pi\, z}{\lambda}\right)\ . \tag{6.3}$$

The range of validity of this formula begins at $z = -\lambda/4$ (where the particle energy is $\mathcal{E}_0$) and continues beyond $z = \lambda/4$ as long as the particle remains in the standing wave. A particular value that will be needed below is

$$\Delta\mathcal{E}_{\rm dr} = \mathcal{E}\left(-\frac{\lambda}{8}\right) - \mathcal{E}\left(-\frac{\lambda}{4}\right) = 0.0908\Delta\mathcal{E}\ . \tag{6.4}$$

This is the energy gain given by Eq. (6.3) in each drift section outside the "effective cavity" of our uniform acceleration model.

Before including any true transverse force the transverse equation of motion for, say, x can be obtained from Eq. (2.8);

$$\frac{d^2x}{dz^2} = -\frac{d\mathcal{E}/dz}{\mathcal{E}}\frac{dx}{dz}\ . \tag{6.5}$$

Solving this equation numerically would yield a result more accurate than Eq. (2.10). Still more accurate is to include the transverse force given by Eq. (5.4);

$$cp\,\frac{d^2x}{dz^2} = F_x = \frac{x\,k_{\rm RF}}{2}\frac{4\Delta\mathcal{E}}{\lambda}\sin 2k_{\rm RF}z \tag{6.6}$$

Augmenting Eq. (6.5) by this term yields

$$\frac{d^2x}{dz^2} = -\frac{d\mathcal{E}/dz}{\mathcal{E}}\,\frac{dx}{dz} + x\,\frac{4\pi}{\lambda^2}\,\frac{\Delta\mathcal{E}}{\mathcal{E}}\,\sin\frac{4\pi\,z}{\lambda}\ . \tag{6.7}$$

Like Eq. (6.3) this formula remains valid as long as the particle remains in the standing wave. Since Eqs. (6.5) and (6.7) are linear, the evolution they describe from input to output can be described by conventionally-defined transfer matrices of the form

$$\mathbf{M} = \begin{pmatrix} C & S \\ C' & S' \end{pmatrix}\ . \tag{6.8}$$

7. Thin Lens Model

To avoid the need for integrating Eq. (6.7) numerically, a thin lens approximation can be used.[8] The transverse momentum imparted to the particle as it traverses the entrance half-cell is

$$\Delta p_r = \int_{-\lambda/4}^{0} F_r\,\frac{dz}{c} = \frac{e\,r\,\hat{E}_{z,\phi}}{2c} = -\frac{r\,\langle\mathcal{E}'_\phi\rangle}{c}\ . \tag{7.1}$$

Though this deflection is distributed in z we will treat it as occurring entirely at the entrance plane. To do this we revert to the $E_z = E_{z,\mathrm{unif.},\phi}$ model in which the radial force is reduced to the sum of two delta functions one at the "effective entrance" one at the "effective exit". Specializing, for example, to horizontal motion, the angular deflection on entry is given by

$$\Delta x' = \frac{\Delta\,(cp_x)}{\mathcal{E}_0} = -x\,\frac{\langle\mathcal{E}'_\phi\rangle}{\mathcal{E}_0}\ . \tag{7.2}$$

This deflection and the corresponding output deflection can be approximated by thin lenses, q_0 on entry and q_1 on exit;†

$$q_{0,1} = \frac{\Delta x'_{0,1}}{x} = \mp\frac{\langle\mathcal{E}'_\phi\rangle}{\mathcal{E}_{0,1}}\ . \tag{7.3}$$

† Formula Eq. (7.3) for quad strengths contain a a factor of 2 (increase) relative to Eq.(12) of Rosenzweig and Serafini (R and S). This is presumably because their assumed field is uniform throughout the entire structure while mine is a train of dentils with duty factor one half. I am at a loss to understand their comment "It should be emphasized that this result applies only to the *secular* portion of the trajectory. If one is concerned with the actual angular deflection of the particle ... (for example the emittance diluting deflection of particles leaving an RF gun) then the results ... should be applied." In any case R and S proceed to employ the result as if it *is* valid. The R and S word definition of $\mathcal{E}'$ (or rather their $\gamma' mc^2$) is "the gradient in the particle energy averaged over a period of the structure". This will be discussed further below.

The vertical motion can be represented similarly with lenses of the same strengths. Note though that, unlike quadrupole magnets, both input lenses are focusing and both exit lenses are defocusing. Approximating the final term of Eq. (6.7) with uniformly-spaced, alternating-sign delta functions, one obtains

$$\frac{d^2x}{dz^2} = -\frac{d\mathcal{E}/dz}{\mathcal{E}}\,\frac{dx}{dz} + \langle\mathcal{E}'\rangle \sum_{n=0}^{\infty} \left(-\frac{\delta\,(z - z_{n0})}{\mathcal{E}_{n,0}} + \frac{\delta\,(z - z_{n1})}{\mathcal{E}_{n,1}} \right) x \ , \tag{7.4}$$

provided that $\mathcal{E}$ increases properly from cell to cell, and according to Eq. (2.6) within cells.

All that remains is to establish the entrance and exit locations z_0 and z_1. Till now these points have been tentatively visualized as being located half way between nodes and cavity center, but it is possible to improve the model somewhat by locating these points more carefully. Their positions can be determined by a centroid-like calculation in which the position is weighted by the deflection angle

$$z_0 = \frac{\int_{-\lambda/4}^{0} z\,\frac{\sin(4\pi z/\lambda)}{\mathcal{E}(z)}\,dz}{\int_{-\lambda/4}^{0} \frac{\sin(4\pi z/\lambda)}{\mathcal{E}(z)}\,dz} \ . \tag{7.5}$$

Except for the z-dependent energy variation, symmetry would yield $z_0 = -\lambda/8$. Since the correction given bt Eq. (7.5) turns out to be insignificant numerically, I will use the symmetric locations $z_{0,1} = \mp\lambda/8$. This result was already used (in parenthesis) in Eq. (2.12).

8. Transfer Matrix Representation

The effects of these entry and exit edge elements can be represented by transfer matrices

$$\mathbf{M}_0 = \begin{pmatrix} 1 & 0 \\ -\frac{\langle\mathcal{E}'_\phi\rangle}{\mathcal{E}_0+\Delta\mathcal{E}_{\rm dr}/2} & 1 \end{pmatrix}, \quad \mathbf{M}_1 = \begin{pmatrix} 1 & 0 \\ \frac{\langle\mathcal{E}'_\phi\rangle}{\mathcal{E}_1-\Delta\mathcal{E}_{\rm dr}/2} & 1 \end{pmatrix} , \tag{8.1}$$

where on-crest, $\phi = 0$, operation has been assumed, and where the energy denominators have been adjusted using Eq. (6.4). (This improves appreciably the match to the exact orbit.) The logarithmic trajectory, the entrance and exit focusing, and the entry and exit drifts can be combined into a single transfer matrix;

$$\mathbf{M} = \begin{pmatrix} 1 & \lambda/8 \\ 0 & 1 \end{pmatrix} \begin{pmatrix} 1 & 0 \\ \frac{\langle\mathcal{E}'\rangle}{\mathcal{E}_1-\Delta\mathcal{E}_{\rm dr}/2} & 1 \end{pmatrix} \begin{pmatrix} 1 & L_{\rm eff.} \\ 0 & \frac{\mathcal{E}_0}{\mathcal{E}_1} \end{pmatrix} \begin{pmatrix} 1 & 0 \\ -\frac{\langle\mathcal{E}'\rangle}{\mathcal{E}_0+\Delta\mathcal{E}_{\rm dr}/2} & 1 \end{pmatrix} \begin{pmatrix} 1 & \lambda/8 \\ 0 & 1 \end{pmatrix} . \tag{8.2}$$

For comparison with other formalisms we drop the edge-lens strength refinement (mentioned below Eq. (8.1)) and multiply the three interior matrices

$$\mathbf{M} = \begin{pmatrix} 1 & \lambda/8 \\ 0 & 1 \end{pmatrix} \begin{pmatrix} 1 - \frac{\langle\mathcal{E}'\rangle}{\mathcal{E}_0}\,L_{\rm eff.} & L_{\rm eff.} \\ -\frac{\langle\mathcal{E}'\rangle^2}{\mathcal{E}_1\mathcal{E}_0}\,L_{\rm eff.} & \frac{\mathcal{E}_0}{\mathcal{E}_1}\left(1 + \frac{\langle\mathcal{E}'\rangle}{\mathcal{E}_0}\,L_{\rm eff.}\right) \end{pmatrix} \begin{pmatrix} 1 & \lambda/8 \\ 0 & 1 \end{pmatrix} . \tag{8.3}$$

In our standing wave model this matrix describes transverse propagation from one node to the next. The outer drifts can be subsumed into adjacent drifts. The effective length of the central "effective cavity" section is

$$L_{\text{eff.}} = \frac{1}{2}\frac{\mathcal{E}_0}{\langle\mathcal{E}'\rangle}\ln\frac{\mathcal{E}_{1,0}}{\mathcal{E}_0} = \frac{1}{2}\frac{\mathcal{E}_0}{\langle\mathcal{E}'\rangle}\ln\left(1+\frac{\langle\mathcal{E}'\rangle\,\lambda/2}{\mathcal{E}_0}\right) = \frac{\lambda}{4} - \dots\,, \tag{8.4}$$

For off-crest operation the second term of Eq. (7.1) can be approximated by a "comb" of alternately focusing and defocusing thin lenses with strengths equal to the edge quads except for the factor $\tan\phi$. Since the edge lenses themselves are fairly weak, and near to on-crest operation is to be expected, I will ignore these lenses. If, for some reason, such as bunch shortening, operation at large ϕ becomes necessary, one should include these lenses.

9. Numerical Investigation of Nine-Cell ERL Front End Section

The transfer matrix given by the R and S model for the entrance face of the first nine-cell ERL is

$$\begin{pmatrix} 1 & 0 \\ -1.0022\,\mathrm{m}^{-1} & 1 \end{pmatrix} \tag{9.1}$$

in both planes. Because of the strongly divergent beam at this point, such a strong lens, focusing in both planes, focal length of one meter, is just what the docter ordered for this position in the linac. Unfortunately, as I have argued, it is bogus to include this lens, without including all subsequent similar lenses. If one *does* include it, neglect interior lens, and include the eventual exit lens (which is given by

$$\begin{pmatrix} 1 & 0 \\ 0.3254\,\mathrm{m}^{-1} & 1 \end{pmatrix}\,,) \tag{9.2}$$

the complete R and S transfer matrix through the nine-cell section is

$$\begin{pmatrix} 0.4375 & 0.5612 \\ -0.1830 & 0.5072 \end{pmatrix}\,. \tag{9.3}$$

The "more nearly correct" (according to Eq. (8.2)) transfer matrix is

$$\begin{pmatrix} 0.3582 & 0.5421 \\ -0.2893 & 0.4686 \end{pmatrix}\,. \tag{9.4}$$

The "exact"† transfer matrix (obtained by numerical integration of orbit equation (6.7)) is

$$\begin{pmatrix} 0.3749 & 0.5461 \\ -0.2671 & 0.4768 \end{pmatrix}\,. \tag{9.5}$$

† Since space charge forces have not been included, "exact" is certainly an overstatement.

Most of the disagreement comes from the very first cell. Comparisons of matrix elements evaluated by "exact", thin lens, and R and S models, through the first four sections, are given in Table 9.1. Exact evolution of the transfer matrix elements through the first nine-cell section is shown in Fig. 9.1.

Table 9.1: Transfer matrix elements through ERL RF 9-cell units. "Exact" implies numerical integration of Eq. (6.7), "thin lens" implies Eq. (8.2), "R and S" implies the Rosenzweig and Serafini "uniform with end lenses" model.

Section	Model	C	S	C'	S'
1	exact	0.3749	0.5461	-0.2671	0.4768
	thin lens	0.3582	0.5421	-0.2893	0.4686
	R and S	0.4375	0.5612	-0.1830	0.5073
2	exact	0.7269	0.7885	-0.0747	0.7401
	thin lens	0.7228	0.7872	-0.0814	0.7372
	R and S	0.7420	0.7929	-0.0501	0.7509
3	exact	0.8239	0.8698	-0.0351	0.8280
	thin lens	0.8221	0.8692	-0.0382	0.8265
	R and S	0.8306	0.8719	-0.0234	0.8334
4	exact	0.8699	0.9110	-0.0203	0.8717
	thin lens	0.8689	0.9107	-0.0222	0.8708
	R and S	0.8737	0.9122	-0.0135	0.8749

10. Reconciliation With Rosenzweig-Serafini Formalism

Entrance and exit focusing formulas (8.1) are close to, but not identical to, formula (12) of Rosenzweig and Serafini. The R and S off-diagonal element (i.e. the inverse focal length) is half as great as mine. Accepting one factor of 2 (the one explained in a footnote on page 12) I can begin to reconcile this by noting that the separation of their entrance and exit edges (being situated at extreme cavity edges) would be twice as great as mine for a single cavity. When the fractional energy gain is small compared to one (which both formalisms require) the entrance plus exit lenses form a doublet. Since "doublet strength" is proportional to lens strength times lens separation, the doublet strength implied by Eq. (8.1) is approximately the same as that given by R and S.

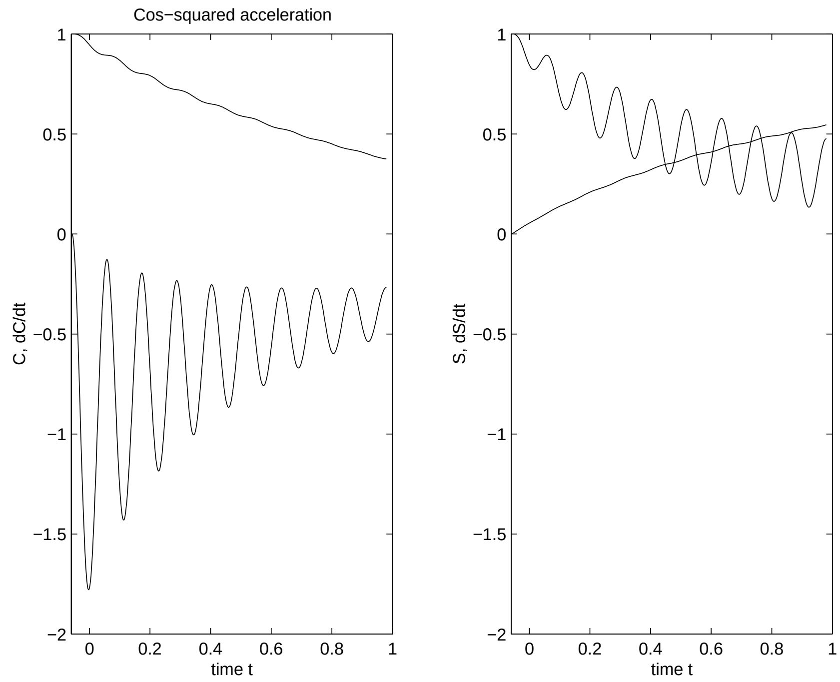

Figure 9.1: Evolution of the "exact" (space charge neglected) transfer matrix elements obtained by numerical integration of trajectory Eq. (6.7). Matrix elements C, S, C', and S' are defined in Eq. $(A.1)$.

This can only be a partial explanation however, as their formula purports to apply to multicell cavities, with end focusing only at the extreme ends. The point here is that they assume a truly uniform longitudinal field. If this were a realistic field there would be no "edges" in the interior, and it would be correct to include no edge lenses in the interior. But the actual longitudinal field, as Fig. 2.1 shows, more nearly resembles my train of dentils and there is already a defocusing lens at the end (actually before the end) of the first node-to-node section. There is a strong tendency for this lens to cancel the first lens. Of course, at the very front end of a linac, the fractional energy gain per multicell section is quite large so, even apart from their finite separation Δz, these lenses do not quite cancel. The approach I advocate, of representing entrance and exit separately at $1/4$ and $3/4$ locations of each node-to-node section, is intended to extend the range of validity to lower energy. I expect the leading defect of this approach is that the very end field is not quite the same as the intracavity transition fields in the interior.

The central "effective cavity" matrix of Eq. (8.3) can be compared with Rosenzweig and Serafini's Eq.(13) (transcribed, and with $\Delta\phi = 0$ and $\eta = 1$)[†]

$$\begin{pmatrix} \cos\alpha - \sqrt{2}\,\sin\alpha & \sqrt{8}\,\frac{\mathcal{E}_0}{\langle\mathcal{E}'\rangle}\sin\alpha \\ -\frac{\langle\mathcal{E}'\rangle}{\mathcal{E}_{1,0}}\,3\sqrt{\frac{1}{8}}\,\sin\alpha & \frac{\mathcal{E}_0}{\mathcal{E}_{1,0}}\left(\cos\alpha + \sqrt{2}\,\sin\alpha\right) \end{pmatrix} \tag{10.1}$$

where

$$\alpha = \frac{1}{\sqrt{8}}\ln\frac{\mathcal{E}_{1,0}}{\mathcal{E}_0} = \frac{1}{\sqrt{8}}\ln\left(1 + \frac{\langle\mathcal{E}'\rangle\,L}{\mathcal{E}_0}\right) = \frac{1}{\sqrt{8}}\left(\frac{\langle\mathcal{E}'\rangle\,L}{\mathcal{E}_0} + \dots\right)\,.$$

In the small α limit (the limit in which it is most nearly valid) this matrix reduces to

$$\begin{pmatrix} 1 - \frac{1}{2}\,\ln\left(1 + \frac{\langle\mathcal{E}'\rangle L}{\mathcal{E}_0}\right) & \frac{\mathcal{E}_0}{\langle\mathcal{E}'\rangle}\,\ln\left(1 + \frac{\langle\mathcal{E}'\rangle L}{\mathcal{E}_0}\right) \\ -\frac{\langle\mathcal{E}'\rangle}{\mathcal{E}_{1,0}}\,\frac{3}{8}\,\ln\left(1 + \frac{\langle\mathcal{E}' L\rangle}{\mathcal{E}_0}\right) & \frac{\mathcal{E}_0}{\mathcal{E}_{1,0}}\left(1 + \frac{1}{2}\,\ln\left(1 + \frac{\langle\mathcal{E}' L\rangle}{\mathcal{E}_0}\right)\right) \end{pmatrix}$$

One sees that there is *essential* agreement between thin lens and R and S models in this limit. The predominant factors $\mathcal{E}_0/\mathcal{E}_{1,0}$ are identical and, in the R and S formalism one would substitute $L = \lambda/2$ for what I have called one "cavity" so their logarithmic factors become equal to my corresponding factors. The remaining discrepancies are fairly minor and are ascribable to my introduction of the "effective cavity" which is half the R and S cavity length, or rather to the end drifts by which the matrices differ.

One sees that the "ponderomotive focusing" of Hartman and Rosenzweig is nowhere to be seen in the matrix for a single cavity. (Eq. (10.1).) To the extent such focusing is important it is will be reconstructed from "alternating gradient focusing" when the single cell matrices are concatenated to produce a multiple-cell transfer matrix.

11. Injection Optics of the Cornell ERL

The only important disagreement between Fig. 1.1 and Fig. 1.2 concerns the values of the α and β lattice functions in the region beginning at the junction between transfer line output and linac input and ending after one or two nine-cell accelerating sections. In this region the electron energy increases from 10 Mev to 30 or 50 MeV. Because of nonrelativistic and space charge complications, the problem of predicting and adjusting these quantities through the gun region, based on the parameters of laser, cathode and

[†] R and S state that transfer matrix (10.1) is "identical to the result obtained previously by Chambers (Stanford HEPL 1969 report)". I don't see how Chamber's 1969 result can contain Hartman and Rosenzweig's "ponderomotive focusing", which they newly introduced in 1993.

gun, is overwhelmingly more difficult than the calculations that have been described. This can only be done numerically and, eventually, empirical tuning is likely to be required to obtain adequate performance. But, for purposes of this report, I assume that arbitrary α and β functions can be achieved out of the gun. This was assumed in tuning up both configurations Fig. 1.1 and Fig. 1.2.

I have only a partial understanding of the assumptions going into Fig. 1.1. I believe though, that Eq. (10.1) has been applied to full nine-cell sections (as if the acceleration is uniform through the full length) rather than as nine separate cells. This optics takes advantage of a highly desirable (but unphysical) lens, at the entrance face of the first cavity, that focuses in both planes, and is strong because the electron energy is minimum at that point. I argue that it is unphysical to include this focusing lens without including also a defocusing lens located at the exit of the same cell. After this issue has been resolved (and all quad strengths made equal) the injection Twiss parameters (given in the captions to Fig. 1.1 and Fig. 1.2) should come into much better agreement.

I believe that Ivan has now developed a more reliable treatment of propagation through the injector. A new comparison is therefore called for, but has not yet been performed. The following section compares calculations through the remainder of the ERL, where the agreement between methods is excellent.

12. Optics of the Rest of the Cornell ERL

Optics within the linac, both for acceleration and deceleration has been exhibited in Fig. 1.2. Twiss functions for the matching section between linac and arc are shown in Fig. 12.1. For the starting portion of the triple bend achromatic region the Twiss functions are shown in Fig. 12.2 and the dispersion in the same region is in Fig. 12.3. Optics for the full ring, not including the far straight section, is shown in Fig. 12.4. All these are in excellent agreement with Bazarov's results.

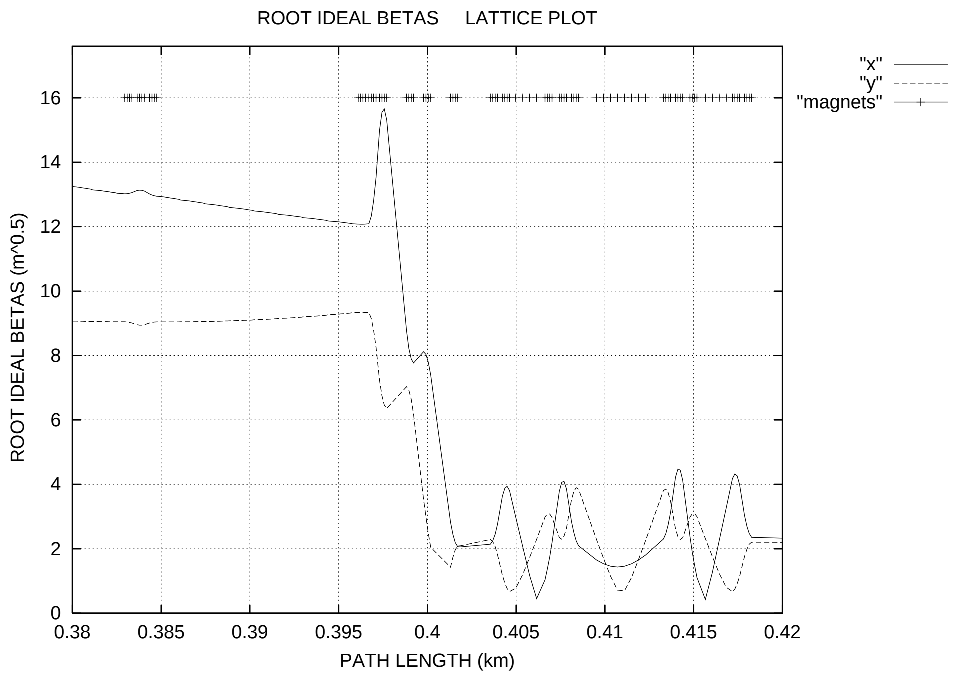

Figure 12.1: Twiss functions in the matching section from linac to arc.

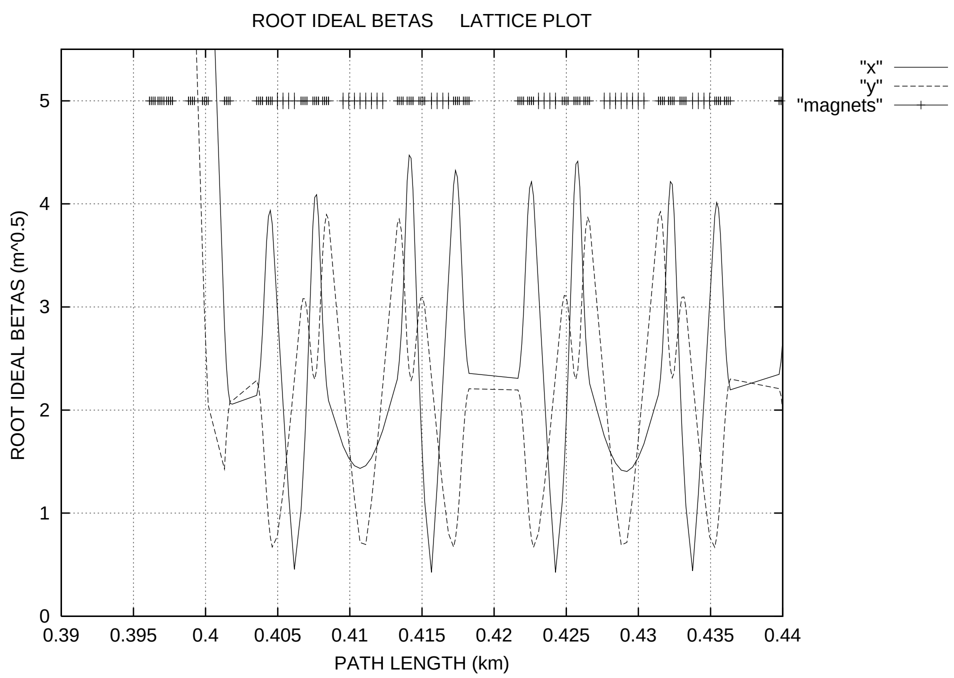

Figure 12.2: Twiss functions near the beginning of the triple bend achromatic turnaround arc.

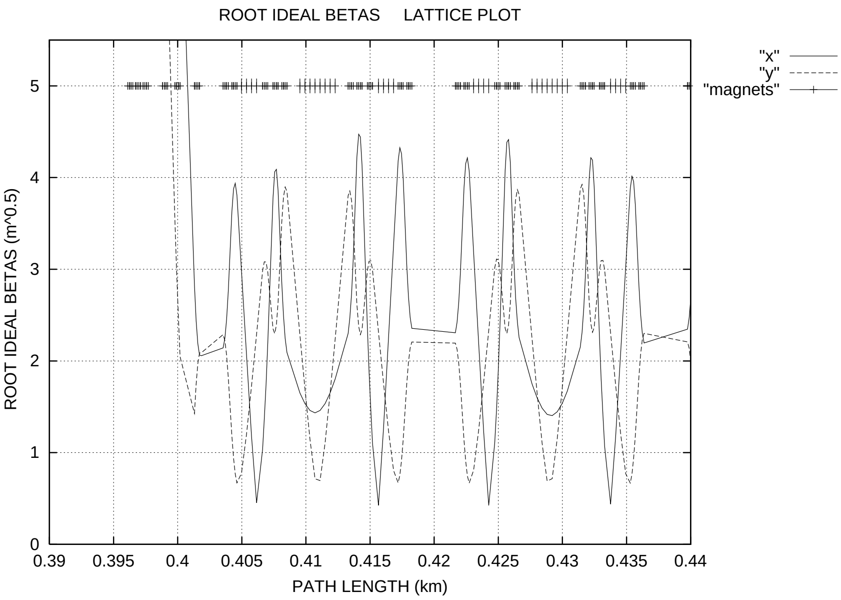

Figure 12.3: Dispersion function near the beginning of the triple bend achromatic turnaround arc.

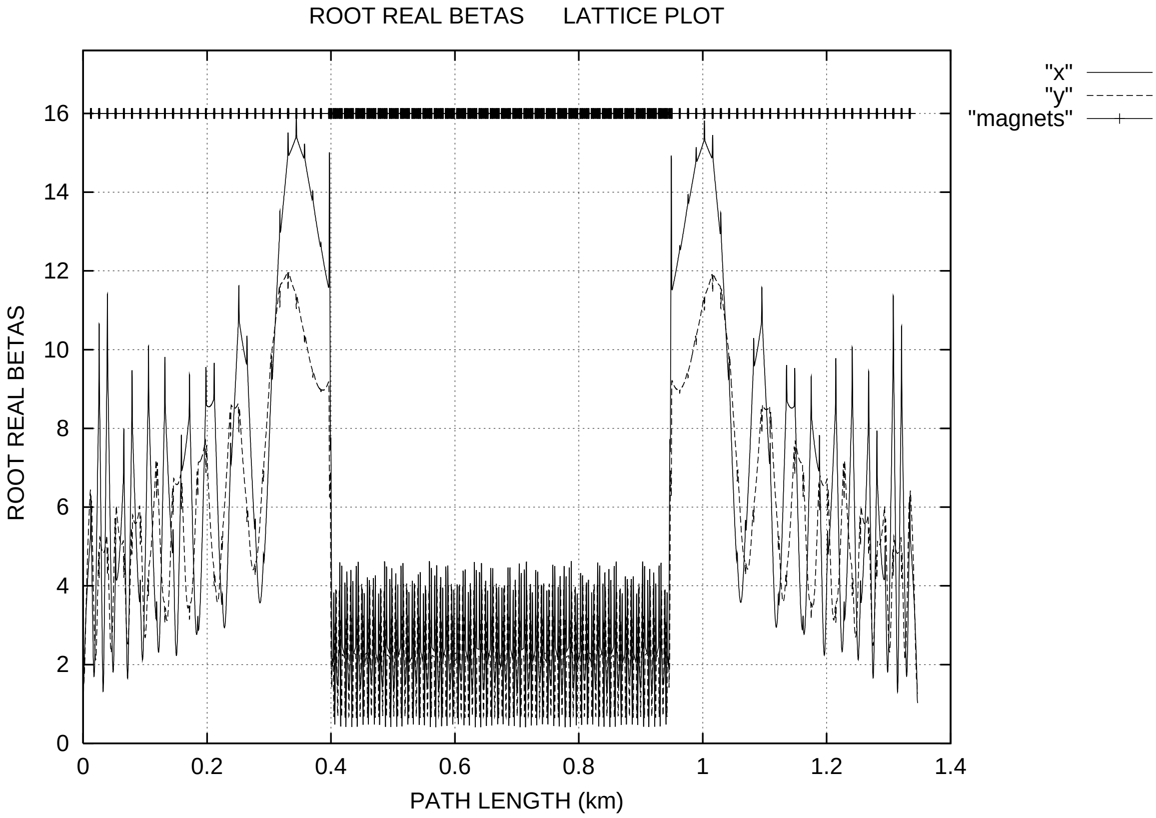

Figure 12.4: Matched optics for the full ERL ring, minus the far straight section.

A. Appendix A. Implementation in TEAPOT

Since TEAPOT does not work with transfer matrices, the transfer matrices derived in earlier sections cannot be applied directly. In particular, drift lengths in TEAPOT have to correspond exactly to the actual distances between elements. This means that $L_{\text{eff.}}$ (effective length) approximations cannot be employed directly. On the other hand the entrance and exit focusing can be modeled by multipole planes which differ from thin quadrupoles only by having *type=slnd* which causes their focus/defocus character to be the same in both planes. Also the sections separating cavity "dentils" can be modeled as standard drifts. It is therefore only the dentil accelerating section transfer matrix that requires special treatment.

Taken at face value (and hence wrong) the transfer matrix given by Rosenzweig and Serafini can be applied to a multicell cavity, since it is only the cavity length and energy gain that enters their formula. The TEAPOT model is less ambitious (more numerical) since it has to break a multicell structure into node-to-node sections, each described by a matrix of the form (8.3), and separated by drifts. The worst case errors can be estimated from the uppermost entries in Table 9.1.

As well as explaining how TEAPOT has been modified other possible consistent treatments of the adiabatic variation of Courant-Snyder variables are considered; for example in a popular linac code PARMELA.

A.1. Twiss Parameters in Energy-Variable Version of TEAPOT

Until these modifications to allow for acceleration were included, TEAPOT determined the Twiss parameters at the origin by reading them off from the once-around storage ring map written in canonical form. From now on it will be possible to enter the Twiss parameters at the origin via the *analysis* command. If they are not entered the code defaults to its previous performance.† Apart from the need to alter the input in this way it is necessary to resolve ambiguity as to how the "Twiss parameters" are defined. To reduce the chances

† There is a subroutine "twiss" in TEAPOT that derives Twiss parameters from the once around transfer matrix. This routine is predicated on the assumption that the ring forms one period of a periodic structure. If there is net acceleration in the ring this assumption is not valid so the subroutine must not be called for open lattices. If there is acceleration, but no *net* acceleration, as in an ERL, the subroutine performs correctly.

for ambiguity I will refrain (to the extent possible) from defining new symbols over and above those currently employed in TEAPOT documentation.

The transfer matrix from point 0 to point 1 is

$$\begin{pmatrix} x_1 \\ x_1' \end{pmatrix} = \mathbf{M} \begin{pmatrix} x_0 \\ x_0' \end{pmatrix} \equiv \begin{pmatrix} C & S \\ C' & S' \end{pmatrix} \begin{pmatrix} x_0 \\ x_0' \end{pmatrix} . \tag{A.1}$$

Though TEAPOT was coded originally under the assumption that the particle energy is conserved, let us now assume that the code has been modified so that the evolution of x is correctly calculated even with acceleration present. Since TEAPOT determines the elements of $\mathbf{M}$ by numerical differentiation;

$$\begin{aligned} C &= \frac{dx_1}{dx_0}, \quad S = \frac{dx_1}{dx_0'}, \\ C' &= \frac{dx_1'}{dx_0}, \quad S' = \frac{dx_1'}{dx_0'}, \end{aligned} \tag{A.2}$$

these coefficients would therefore be calculated correctly. (Though the primes on C' and S' originally denoted s-derivatives, this will not necessarily remain the case in the presence of energy variation.)

While particle energy was assumed to remain constant the phase ellipse at location i was defined by†

$$\epsilon_i = \Gamma_i x_i^2 + 2\alpha_i x_i x_i' + \beta_i x_i'^2 \stackrel{?}{=} \frac{x_i^2 + (\alpha_i x_i + \beta_i x_i')^2}{\beta_i} . \tag{A.3}$$

where the latter rearrangement followed from the relation

$$\Gamma_i = \frac{1+\alpha_i^2}{\beta_i}, \quad \text{(which may no longer be valid)} \tag{A.4}$$

but which follows if and only if $\det|\mathbf{M}| = 1$.

When the energy is allowed to vary (because of RF elements) ϵ_i no longer remains constant, but let us assume that the phase space coordinates x, x' remain on an ellipse, and that $(A.3)$ (first equation) continues to be the equation of this ellipse. Because of energy variation ϵ_i will no longer be constant. Rather

$$\epsilon_i = \frac{\bar{\epsilon}}{\gamma_i}, \tag{A.5}$$

† For the time being the third Twiss parameter will be called Γ instead of the conventional γ. This is to avoid serious confusion when the relativistic factor γ is introduced. As soon as the relation $\Gamma = (1+\alpha^2)/\beta$ is understood in the (new) context of energy variation, Γ will be eliminated in favor of α and β.

where $\bar{\epsilon}$, the "normalized emittance" *is* constant. With transformation $(A.1)$ this will determine the evolution of the Twiss parameters.

Phase space areas transform proportional to the Jacobian of the transformation, which is $CS' - SC'$, and (assuming adiabatic variation) it is known that the phase space area is proportional to $1/\gamma$. It follows that

$$\det|\mathbf{M}| = \frac{\gamma_0}{\gamma}, \quad \text{and hence} \quad \mathbf{M}^{-1} = \frac{\gamma}{\gamma_0}\begin{pmatrix} S' & -S \\ -C' & C \end{pmatrix} . \tag{A.6}$$

We are requiring the ellipse equation at the origin to take the form

$$\Gamma_0 x_0^2 + 2\alpha_0 x_0 x_0' + \beta_0 {x_0'}^2 = \frac{\bar{\epsilon}}{\gamma_0} , \tag{A.7}$$

and the evolving equation to have the same form (without the 0 subscripts.) Under transformation $(A.1)$, quadratic form $\Gamma_0 x_0^2 + 2\alpha_0 x_0 x_0' + \beta_0 {x_0'}^2$ transforms to quadratic form $\Gamma x^2 + 2\alpha x x' + \beta_0 {x'}^2$ with coefficients given by

$$\begin{pmatrix} \Gamma & \alpha \\ \alpha & \beta \end{pmatrix} = \left(\mathbf{M}^{-1}\right)^T \begin{pmatrix} \Gamma_0 & \alpha_0 \\ \alpha_0 & \beta_0 \end{pmatrix} \mathbf{M}^{-1}, \tag{A.8}$$

so the equation of the new phase space ellipse is

$$\Gamma x^2 + 2\alpha x x' + \beta {x'}^2 = \frac{\bar{\epsilon}}{\gamma_0} , \tag{A.9}$$

which differs from what we want only by a factor γ_0/γ missing from the right hand side. Allowing for this factor and completing the multiplications in Eq. $(A.8)$ we obtain

$$\begin{pmatrix} \beta \\ \alpha \\ \Gamma \end{pmatrix} = \frac{\gamma}{\gamma_0}\begin{pmatrix} C^2 & -2CS & S^2 \\ -CC' & CS' + SC' & -SS' \\ {C'}^2 & -2C'S' & {S'}^2 \end{pmatrix}\begin{pmatrix} \beta_0 \\ \alpha_0 \\ \Gamma_0 \end{pmatrix} \tag{A.10}$$

For example

$$\beta = \frac{\gamma}{\gamma_0}\left(\left(\frac{dx}{dx_0}\right)^2 \beta_0 - 2\frac{dx}{dx_0}\frac{dx}{dx_0'}\alpha_0 + \left(\frac{dx}{dx_0'}\right)^2 \Gamma_0\right) \tag{A.11}$$

This differs only by the factor γ/γ_0 from the formula used to propagate β in the original, constant-energy version of TEAPOT. This is *essentially* how ftpotERL† has been modified

† The changes needed to account for acceleration are minor enough that the revised version, temporarily called "ftpotERL" has been coded to be backward compatible with the previous version. But the test suite has not been run to confirm this.

to account for energy variation. But it turned out to be easier to modify the transfer matrix according to†

$$\begin{pmatrix} C & S \\ C' & S' \end{pmatrix} \to \begin{pmatrix} r_\gamma C & r_\gamma S \\ r_\gamma C' & r_\gamma S' \end{pmatrix}, \quad \text{where} \quad r_\gamma = \sqrt{\frac{\gamma}{\gamma_0}}. \tag{A.12}$$

This restores the equality $|\det \mathbf{M}| = 1$.

A candidate (but in the end not adopted) fix for TEAPOT would have been to recognize that it is more symmetric to write Eq. (A.10) in the form

$$\begin{pmatrix} \beta/\gamma \\ \alpha/\gamma \\ \Gamma/\gamma \end{pmatrix} = \begin{pmatrix} C^2 & -2CS & S^2 \\ -CC' & CS' + SC' & -SS' \\ C'^2 & -2C'S' & S'^2 \end{pmatrix} \begin{pmatrix} \beta_0/\gamma_0 \\ \alpha_0/\gamma_0 \\ \Gamma_0/\gamma_0 \end{pmatrix}. \tag{A.13}$$

Then, instead of entering $\beta_0, \alpha_0, \Gamma_0$ one would have entered $\beta_0/\gamma_0, \alpha_0/\gamma_0, \Gamma_0/\gamma_0$. With no further internal changes to TEAPOT (other than correctly calculating the evolution of x and x' plus points to be mentioned momentarily) the code would then output $\beta/\gamma, \alpha/\gamma, \Gamma/\gamma$ from which the γ could be factored out to obtain the lattice functions. In following this procedure it would be important to treat Γ consistently. We would have

$$\Gamma_0 = \frac{1+\alpha_0^2}{\beta_0}, \quad \text{and} \quad \Gamma = \frac{1+\alpha^2}{\beta}, \tag{A.14}$$

but the relations among the components of the vectors appearing in Eq. (A.13) are more complicated and depend on γ. Apart from this consideration, the reason this fix was not adopted is that (naturally) the Twiss parameters are scattered throughout the code, with names that are not particularly consistent, and their names suggest their interpretations as *geometric* (a term defined below) Twiss parameters. It would be highly misleading to leave these names unchanged and a nightmare to change them. Furthermore the numerical values of the *normalized* (a term defined below) Twiss parameters, altered by a large γ-factor, lose the mnemonic value that is attached to the familiar geometric Twiss parameters. The fix for TEAPOT will be to keep the Twiss parameters current at every energy by incorporating factors such as γ/γ_0 in equations such as (A.10) when the Twiss parameters are being updated.

† The 2x2 matrix elements are calculated only in subroutine "matget" and only from the origin to particular elements that are indexed by $ielem = 0, 1, ..., nelem$. "matget" works only from the array "trtrout(i, ipart)" where $i = 1, 2, ..., 6$ is the displacement vector index and $ipart = 1, 2, ..., 20$ is the particle index. The amplitudes at the origin are TEAPOT inputs xtyp, pxtyp, ytyp, pxtyp. The element index is implicit (i.e. it is not an explicit argument in the call to matget()). We therefore obtain the desired effect by multiplying every spatial element ($i = 1, 2, 3, 4$) of trtrout(i, ipart) by $\sqrt{\gamma/\gamma_0}$. The 4x4 analysis starts with a call to "gettunrt" which is useless for open lattices.

The Twiss parameters also appear in what Sands calls the "pseudoharmonic" description of betatron oscillations. As defined so far, the equation of the phase space ellipse is

$$\frac{x^2 + (\alpha x + \beta x')^2}{\beta} = \frac{\bar{\epsilon}}{\gamma}\ . \tag{A.15}$$

In this form we recognize the possibility of "circular" phase space description with coordinates $x, \alpha x + \beta x'$, in terms of which Eq. (A.15) is the equation of a circle. Introducing ψ (or, if one prefers, $\psi - \psi_0$) as the angle subtended at the origin by a point on this circle and solving for x', we obtain

$$x = \sqrt{\frac{\beta\bar{\epsilon}}{\gamma}}\cos\psi, \quad x' = -\sqrt{\frac{\bar{\epsilon}}{\beta\gamma}}\,(\sin\psi + \alpha\cos\psi) \tag{A.16}$$

as evolving phase space coordinates. (Though $\bar{\epsilon}$ is usually thought to be a beam property (emittance) it is now being used as a particle property (Courant-Snyder invariant) but this distinction should not affect transformation properties. We can think of $\bar{\epsilon}$ as belonging to a particular particle whose Courant-Snyder is equal to the beam emittance.)

It is a challenge to be certain that the Twiss definitions described up to this point conform with other people's definitions. One feature is clear. At a point in the lattice at which $\alpha = 0$, the semi-major axis of the phase space ellipse with Cartesian coordinates x, x' is $\sqrt{\beta\epsilon}$ and the semi-minor axis is $\sqrt{\epsilon/\beta}$. Therefore β is the aspect ratio (major/minor) of the ellipse provided that x, x' coordinates are used. Changing the scales by a constant factor does not affect this.

Ivan Bazarov tells me that his β-function (which he and others call the "geometric beta function", a terminology I adopt) is defined to be $\beta^{\rm IB}$ as it appears in the equation,

$$x = \sqrt{\beta^{\rm IB}\epsilon}\,\cos\psi. \tag{A.17}$$

It follows from Eqs. (A.5) and (A.16) that $\beta^{\rm IB}$ is the same as the β defined in this note.

PARMELA introduces a different "normalized" beta function which (dropping a dimensionsless numerical factor introduced to account for their non-SI units) satisfies

$$x = \sqrt{\beta_{\rm n}^{\rm PARMELA}\bar{\epsilon}}\,\cos\psi, \tag{A.18}$$

where $\bar{\epsilon}$ is the previously-defined "normalized emittance". With Eq. (A.16), this beta function definition implies

$$\beta_{\rm n}^{\rm PARMELA} = \bar{\beta} = \frac{\beta}{\gamma}. \tag{A.19}$$

It remains to be seen how $\bar{\alpha}$ and $\bar{\Gamma}$ should be introduced to be consistent with Eq. $(A.19)$.

There is another way of defining "normalized phase space". It is to adopt $(\bar{x}, \bar{x}') = (x, \gamma x')$ as phase space coordinates. This approach can even be said to be "more correct" since $\gamma x'$ is the momentum variable conjugate to x in the sense of Hamiltonean mechanics. Let us see where this approach would have taken us.

Preparing to allow γ to vary we rearrange Eq. $(A.1)$ into the form

$$\begin{pmatrix} \bar{x}_1 \\ \bar{x}'_1 \end{pmatrix} = \begin{pmatrix} \bar{C} & \bar{S} \\ \bar{C}' & \bar{S}' \end{pmatrix} \begin{pmatrix} \bar{x}_0 \\ \bar{x}'_0 \end{pmatrix} \equiv \bar{\mathbf{M}} \begin{pmatrix} \bar{x}_0 \\ \bar{x}'_0 \end{pmatrix}, \tag{A.20}$$

where

$$\begin{gathered} \bar{x} = x,\ \bar{x}' = x'\gamma, \\ \bar{C} = C,\ \bar{S} = \frac{S}{\gamma_0}, \\ \bar{C}' = C'\gamma_1,\ \bar{S} = S'\frac{\gamma_1}{\gamma_0}, \end{gathered} \tag{A.21}$$

So far this is just a change of variable and makes no assumption, but it is implicitly assumed that the equations will remain valid when γ varies and, at a minimum, this will require that some sort of "adiabatic" assumption has been made. (e.g. the fractional change in γ is small during one betatron oscillation.) This assumption is likely to break down in the nonrelativistic regime, but other results will also become invalid when the $v \approx c$ assumption breaks down.

Because the phase space area is conserved we have

$$\det|\mathbf{M}| = 1, \quad \text{and hence} \quad \mathbf{M}^{-1} = \begin{pmatrix} S' & -S \\ -C' & C \end{pmatrix} . \tag{A.22}$$

Also we introduce modified Twiss parameters by

$$\bar{\Gamma} = \gamma\Gamma, \quad \bar{\alpha} = \alpha, \quad \bar{\beta} = \frac{\beta}{\gamma}, \quad \bar{\epsilon} = \gamma\epsilon. \tag{A.23}$$

Note that identity $(A.4)$ applies equally well to barred variables, since

$$\bar{\Gamma} = \gamma\frac{1+\alpha^2}{\beta} = \frac{1+\bar{\alpha}^2}{\bar{\beta}}, \tag{A.24}$$

so we will be free to use these relations to eliminate Γ wherever it appears. Performing these changes of variables, the equation of phase ellipse $(A.3)$ becomes

$$\bar{\epsilon} = \bar{\Gamma}_i\bar{x}_i^2 + 2\bar{\alpha}_i\bar{x}_i\bar{x}'_i + \bar{\beta}_i\bar{x}'^2_i = \frac{\bar{x}_i^2 + \left(\bar{\alpha}_i\bar{x}_i + \bar{\beta}_i\bar{x}'_i\right)^2}{\bar{\beta}_i} , \tag{A.25}$$

In this step the index on $\bar{\epsilon}_i$ has been suppressed because $\bar{\epsilon}_i$ is known to be independent of i if the energy is varying adiabatically, as is now being permitted. The same derivation as yielded Eq. ($A.10$) now yields

$$\begin{aligned}\bar{\beta} &= \bar{C}^2\bar{\beta}_0 - 2\bar{C}\bar{S}\bar{\alpha}_0 + \bar{S}^2\bar{\Gamma}_0,\\ \bar{\alpha} &= \;-\bar{C}\bar{C}'\bar{\beta}_0 + \left(\bar{C}\bar{S}' + \bar{S}\bar{C}'\right)\bar{\alpha}_0 - \bar{S}\bar{S}'\bar{\Gamma}_0.\end{aligned} \tag{A.26}$$

On the other hand TEAPOT would continue to determine the derivatives appearing in Eq. ($A.2$) and these could be used to determine the elements of $\bar{\mathbf{M}}$ using Eqs. ($A.21$);

$$\begin{aligned}\bar{C} &= \frac{dx}{dx_0}, \quad \bar{S} = \frac{dx}{dx'_0}\frac{1}{\gamma_0},\\ \bar{C}' &= \frac{dx'}{dx_0}\gamma, \quad \bar{S}' = \frac{dx'}{dx'_0}\frac{\gamma}{\gamma_0},\end{aligned} \tag{A.27}$$

Within TEAPOT Eqs. ($A.26$) would take the form

$$\begin{aligned}\bar{\beta} &= \left(\frac{dx}{dx_0}\right)^2\bar{\beta}_0 - 2\frac{dx}{dx_0}\frac{dx}{dx'_0}\frac{\bar{\alpha}_0}{\gamma_0} + \left(\frac{dx'}{dx'_0}\right)^2\frac{\bar{\Gamma}_0}{\gamma_0^2},\\ \frac{\bar{\alpha}}{\gamma} &= \;-\frac{dx}{dx_0}\frac{dx'}{dx_0}\bar{\beta}_0 + \left(\frac{dx}{dx_0}\frac{dx'}{dx'_0} + \frac{dx}{dx'_0}\frac{dx'}{dx_0}\right)\frac{\bar{\alpha}_0}{\gamma_0} - \frac{dx}{dx'_0}\frac{dx'}{dx'_0}\frac{\bar{\Gamma}_0}{\gamma_0^2}.\end{aligned} \tag{A.28}$$

Let us introduce quantities that purport to be appropriate for entry into and output from TEAPOT:

$$\beta^{\rm tp} = \bar{\beta} = \frac{\beta}{\gamma}, \quad \alpha^{\rm tp} = \frac{\bar{\alpha}}{\gamma} = \frac{\alpha}{\gamma}, \quad \Gamma^{\rm tp} = \frac{\bar{\Gamma}}{\gamma^2} = \frac{1+\left(\gamma\alpha^{\rm tp}\right)^2}{\gamma^2\beta^{\rm tp}} = \frac{\Gamma}{\gamma}\,. \tag{A.29}$$

These have been chosen so that Eq. ($A.28$) becomes

$$\begin{aligned}\beta^{\rm tp} &= \left(\frac{dx}{dx_0}\right)^2\beta_0^{\rm tp} - 2\frac{dx}{dx_0}\frac{dx_1}{dx'_0}\alpha_0^{\rm tp} + \left(\frac{dx'}{dx'_0}\right)^2\Gamma_0^{\rm tp},\\ \alpha^{\rm tp} &= \;-\frac{dx}{dx_0}\frac{dx'_1}{dx_0}\beta_0^{\rm tp} + \left(\frac{dx}{dx_0}\frac{dx'_1}{dx'_0} + \frac{dx_1}{dx'_0}\frac{dx'_1}{dx_0}\right)\alpha_0^{\rm tp} - \frac{dx}{dx'_0}\frac{dx'_1}{dx'_0}\Gamma_0^{\rm tp}.\end{aligned} \tag{A.30}$$

Comparing with Eq. ($A.11$), we see that the original Twiss parameter TEAPOT evolution results will continue to be valid provided we read parameters in and out according to Eqs. ($A.29$). This amounts to the same procedure as in Eq. ($A.13$) for "tricking" TEAPOT by transforming inputs and outputs that was described above (and rejected.)

The only benefit, I can think of, to come from having contemplated multiple possible procedures is that the following hazard has been identified. When TEAPOT was first written, the identity $\Gamma = (1+\alpha^2)/\beta$ was identically true, so it was "hard-wired" into the code in one or more places which would now take the form

$$\Gamma^{\rm tp} = \frac{1+\left(\alpha^{\rm tp}\right)^2}{\beta^{\rm tp}}, \text{ which is incorrect in general.} \tag{A.31}$$

That this is incorrect can by seen by comparing with the last of Eqs. (A.29). For example, since only β and α are input, if γ appears at all internal to TEAPOT, it has undoubtedly been calculated using Eq. (A.31). All such occurrences had to be tracked down and fixed.

A.2. Dispersion

Though the energy increases in linac sections, let us suppose that there are also decelerating sections and that the lattice file returns the energy to its value at the start.† If one pretends that the particle can re-materialize at the beginning and complete another transit, then the lattice file can be subjected to all traditional storage ring analyses. In particular the dispersion function $\eta(0)$ at the origin is that displacement such that a particle launched with energy $p_0(1+\delta)$ at position $\eta(0)\delta$ (with zero slope) returns to the same position. Since, as already stated, the energy returns to its starting value, the unchanged TEAPOT machinery will calculate $\eta(0)$ correctly. (Subroutine *geteta*.)

Because of the changing energy the longitudinal variation, $\eta(s)$, is slightly more complicated. Teapot starts a particle with momentum $p_0(1+\delta_{typ})$ from the position $\eta(0)\delta_{typ}$ and tracks it around the ring; its displacement at position i is $x(s_i)$. Let us assume that the *absolute* energy deviation of this particle is preserved even in the presence of acceleration. Its *relative* energy deviation is therefore proportion to its energy. Starting with the definition of $\eta(s_i)$ one has

$$x\left(s_i\right) = \eta\left(s_i\right)\, \frac{p\left(s_i\right)-p\left(0\right)}{p\left(s_i\right)} = \eta\left(s_i\right)\, \delta_{typ}\, \frac{e\left(s_i\right)}{e\left(0\right)}\ .$$

The final factor has been incorporated into the TEAPOT code. (Subroutine *traeta*.) This has no effect on ordinary storage rings since the final factor reduces to 1.

† Energy and (magnitude of) momentum will be considered equivalent in this section.

References

1. I. Bazarov, ERL-Prototype-TN-01-(001,002,&003), March, 2001, as well as private communication.
2. L. Schachinger and R. Talman, *Particle Accelerators*, **22**, 35 (1897).
3. J. Rosenzweig, S. Hartman, and J. Stevens, 1993 IEEE Accelerator Conference, p. 3357.
4. S. Hartman and J. Rosenzweig, Phys. Rev. E, **47**, 2031 (1993).
5. J. Rosenzweig and L. Serafini, *Transverse particle motion in radio-frequency linear accelerators,* Phys. Rev. E, **49**, 1599 (1994).
6. K-J Kim, N.I.M., **A275**, 201 (989).
7. R. Helm and R. Miller, in *Linear Accelerators*, eds. P. Lapostolle and A. Septier, North Holland, 115 (1989).
8. T. Wangler, *Priciples of RF Linear Accelerators*, John Wiley, 1998, p. 201, ascribes a thin lens model of transverse motion in a cavity to R. L. Gluckstern, private communication.